JGV Papers in Press. Published June 5, 2013 as doi:10.1099/vir.0.054122-0

# Assembly and characterization of foot-and-mouth disease virus empty capsid particles expressed within mammalian cells

Maria Gullberg[1], Bartosz Muszynski[1,§], Lindsey J. Organtini[2], Robert E. Ashley[2], Susan L. Hafenstein[2], Graham J. Belsham[1] and Charlotta Polacek[1,*]

[1]*National Veterinary Institute, Technical University of Denmark, Lindholm, 4771 Kalvehave, Denmark.*

[2]*Department of Microbiology and Immunology, the Pennsylvania State University College of Medicine, 500 University Drive, Hershey, Pennsylvania 17033, USA.*

[§]*Present address: Sheffield Institute for Translational Neurosciences, University of Sheffield, 385a Glossop Road, Sheffield S10 2HQ, United Kingdom.*

*Corresponding author.

Mailing address: National Veterinary Institute, Technical University of Denmark, Lindholm, 4771 Kalvehave, Denmark.

Phone: +45 3588 7881. Fax: +45 3588 7901. E-mail: chapo@vet.dtu.dk.

Running title: Assembly and properties of FMDV empty capsids

Summary word count: 237

Text word count: 5500

Figures: 6

Supplementary Table: 1

**Summary**

The foot-and-mouth disease virus (FMDV) structural protein precursor, P1-2A, is cleaved by the virus-encoded 3C protease ($3C^{pro}$) into the capsid proteins VP0, VP1 and VP3 (and 2A). In some systems, it is difficult to produce large amounts of these processed capsid proteins since $3C^{pro}$ can be toxic for cells. The expression level of $3C^{pro}$ activity has now been reduced relative to the P1-2A, and the effect on the yield of processed capsid proteins and their assembly into empty capsid particles within mammalian cells has been determined. Using a vaccinia virus based transient expression system, P1-2A (from serotypes O and A) and $3C^{pro}$ were expressed from monocistronic cDNA cassettes as P1-2A-3C, or from dicistronic cassettes with the $3C^{pro}$ expression dependent on a mutant FMDV IRES (P1-2A-mIRES-3C). The effects of using a mutant $3C^{pro}$ with reduced catalytic activity or using two different mutant IRES elements (the wild-type GNRA tetraloop sequence GCGA converted, in the cDNA, to GAGA or GTTA) were analysed. For both serotypes, the P1-2A-mIRES-3C construct containing the inefficient GTTA mutant IRES produced the highest amount of processed capsid proteins. These products self-assembled to form FMDV empty capsid particles, which have a related, but distinct, morphology (as determined by electron microscopy and reconstruction) from that determined previously by X-ray crystallography. The assembled empty capsids bind, in a divalent cation-dependent manner, to the RGD-dependent integrin $\alpha_v\beta_{6,}$ a cellular receptor for FMDV, and are recognized appropriately in serotype-specific antigen ELISAs.

**Keywords:** Foot-and-mouth disease virus, 3C protease, empty capsids, capsid assembly, picornavirus.

## Introduction

Foot-and-mouth disease virus (FMDV) is the prototypic member of the *Aphthovirus* genus within the *Picornaviridae*. The virus is responsible for one of the most economically important diseases of livestock including cattle, pigs and sheep plus many different cloven-hoofed wildlife species (Alexandersen *et al.*, 2003; Grubman & Baxt, 2004). As with other picornaviruses, the FMDV particle consists of a single copy of the positive sense RNA genome (ca. 8300 nt) within a protein capsid (Belsham, 2005). This capsid is comprised of 60 copies of 4 different virus proteins VP4 (1A), VP2 (1B), VP3 (1C) and VP1 (1D); the VP4 is internal but each of the other proteins are surface exposed (Acharya *et al.*, 1989). The FMDV proteins are produced from a single large polyprotein that is co-translationally cleaved into precursor proteins (L, P1-2A, P2 and P3) and subsequently into some 15 different mature proteins. The capsid proteins are produced from the P1-2A precursor through the action of the 3C protease ($3C^{pro}$) which processes it to VP0 (1AB), VP3 and VP1 plus the 2A peptide (18 amino acids). Cleavage of VP0 (to VP4 and VP2) occurs on encapsidation of the viral RNA but can also occur more slowly independently from this process (Curry *et al.*, 1997). The P1-2A precursor is modified, by the cellular myristylation system, on its N-terminal gly (G) residue (Chow *et al.*, 1987), following cleavage of the L/P1 junction by the L protease (Medina *et al.*, 1993). The processed FMDV capsid proteins can self-assemble into empty capsid particles (Abrams *et al.*, 1995). Empty capsid particles, generated in FMDV-infected cells, share the same antigenic and immunogenic characteristics as the intact virus but they are not infectious (Rowlands *et al.*, 1975).

Seven distinct serotypes of FMDV are known, namely O, A, C, Asia-1, SAT1, SAT2 and SAT3. There is little or no cross-protection between the different serotypes and sometimes even within a serotype, thus there has to be careful matching between vaccine strains and the viruses involved in disease outbreaks. Serotype O is the most frequently reported virus but some

71 countries have concurrent infections with multiple serotypes (e.g. within Eurasia, serotypes O, A
72 and Asia-1 have circulated recently, see http://www.wrlfmd.org/fmd_genotyping/). The SAT
73 viruses are usually confined to sub-Saharan Africa while serotype C has not been identified from
74 outbreaks for several years.

75 In addition to determining the antigenic properties of the virus, the surface exposed capsid
76 proteins of FMDV are also critical for binding of the virus to cells. The major cellular receptor
77 for FMDV is the integrin $\alpha_v\beta_6$ that is expressed on epithelial cells and binds to an RGDLXXL
78 motif within the VP1 protein (Jackson *et al.*, 2000; Monaghan *et al.*, 2005). During growth in cell
79 culture (e.g. in BHK cells), virus adaptation can occur, e.g. cell culture adapted serotype O
80 viruses can use heparan sulfate as an alternative receptor due to amino acid substitutions within
81 VP3 (Jackson *et al.*, 1996). However, such cell culture adapted viruses can be attenuated in
82 animals (Bøtner *et al.*, 2011; Lohse *et al.*, 2012; Sa-Carvalho *et al.*, 1997).

83 Vaccines against FMD are widely used where the disease is endemic (e.g. within Africa and
84 Southern Asia) and were successful for combatting the disease within Europe in the 1960's/70's.
85 However, now vaccination against FMD is not permitted within the EU except during a disease
86 outbreak and was used in The Netherlands in 2001 (Bouma *et al.*, 2003). Currently, the
87 production of FMDV vaccines requires the growth of large amounts of infectious virus which is
88 then inactivated before use, thus vaccine production plants represent a potential risk for the
89 escape of infectious FMDV (Rodriguez & Grubman, 2009).

90 There has, therefore, been considerable interest in producing empty capsid particles for use as
91 potential vaccines against FMD (Abrams *et al.*, 1995; Cao *et al.*, 2009; Porta *et al.*, 2013a; Porta
92 *et al.*, 2013b). In addition, defective human adenovirus vectors which express the components
93 required for FMDV empty capsid particle formation have been developed (Moraes *et al.*, 2002;
94 Moraes *et al.*, 2011; Pacheco *et al.*, 2005).

There has been some success in using different systems for the production of the FMDV empty capsid particles but there have also been a number of challenges. For example, it has not been possible to isolate single recombinant vaccinia viruses which co-express the P1-2A precursor with the $3C^{pro}$ (Abrams *et al.*, 1995). Furthermore, in the baculovirus expression system, the $3C^{pro}$ has proved to have adverse effects on protein expression (Porta *et al.*, 2013a). This may result from the fact that the FMDV $3C^{pro}$ has a number of cellular targets including certain translation initiation factors (eIF4G and eIF4A, Belsham *et al.*, 2000), cytoskeleton components (Armer *et al.*, 2008) and histone H3 (Falk *et al.*, 1990). Indeed, constitutive expression of FMDV $3C^{pro}$ can only be achieved at low levels in mammalian cells (Martinez-Salas & Domingo, 1995). This has led to attempts to decrease the level of $3C^{pro}$ activity that is co-expressed with the P1-2A precursor and it has been shown that equimolar amounts of the $3C^{pro}$ are not required to achieve efficient processing of the P1-2A within both insect and mammalian cells (Polacek *et al.*, 2013; Porta *et al.*, 2013a; Porta et al., 2013b).

One strategy to reduce the level of $3C^{pro}$ activity is to use mutant forms of this protease with reduced enzymatic activity; such mutants have been described previously (Sweeney *et al.*, 2007). An alternative system relies on reducing the amount of $3C^{pro}$ expression relative to the P1-2A. This can be achieved by differential levels of transcription, e.g. using different promoters to drive the expression of two different cDNA cassettes (as used with enterovirus 71, Chung *et al.*, 2010). Alternatively, a single cDNA cassette containing the coding sequences for FMDV P1-2A and $3C^{pro}$ has been used in insect cells with the two coding sequences being separated by a frame-shift signal (Porta *et al.*, 2013a; Porta *et al.*, 2013b). In addition, two separate open reading frames (ORFs) can be expressed from a single dicistronic mRNA with an inefficient (mutant) internal ribosome entry site (IRES) located between them. The use of a mutant IRES (designated mIRES) can result in relatively low level translation of the downstream ORF (here $3C^{pro}$). In the

current study, alternative systems for the expression and processing of FMDV capsid proteins (from serotypes O and A) within mammalian cells have been analysed. Using the optimal system, efficient assembly of empty capsid particles which bind to the $\alpha_v\beta_6$ integrin and appropriately to serotype-specific anti-FMDV antibodies has been demonstrated.

## Results

*Structure of FMDV cDNA cassettes*

To analyse the expression, processing and assembly of FMDV capsid proteins, FMDV cDNA cassettes derived from serotype O and serotype A viruses were constructed. Schematic representations of these cassettes, all under the control of the bacteriophage T7 promoter, are shown in Fig. 1. The plasmids encode the FMDV structural protein precursor P1-2A alone or with $3C^{pro}$ as either a single ORF (in P1-2A-3C cassettes), or as two separate ORFs within a single RNA transcript with the $3C^{pro}$ expression being dependent on the FMDV IRES (in P1-2A-IRES-3C cassettes). To reduce the level of $3C^{pro}$ activity generated and to determine the optimal system for the co-expression of this protease with the capsid protein precursor, two different strategies were used. Either (i) a mutant $3C^{pro}$ ($3C^{pro}$ C142S), with reduced protease activity (Birtley *et al.*, 2005; Sweeney *et al.*, 2007), was included in the cassettes or (ii) mIRES elements, with reduced ability to direct internal initiation of protein synthesis, were employed to produce the $3C^{pro}$. Previously, it has been shown that the $3C^{pro}$ C142S substitution reduces the activity of $3C^{pro}$ *in vitro* to <1% of the wt protease activity (Sweeney *et al.*, 2007). Two different mIRES elements were designed and constructed based on previous results with the closely related encephalomyocarditis virus (EMCV) IRES (Robertson *et al.*, 1999). This type of IRES contains a highly conserved GNRA tetraloop motif (GCGA in FMDV), which is essential for maximum activity (Roberts & Belsham, 1997; Robertson *et al.*, 1999; Lopez de Quinto & Martinez-Salas,

1997; Fernandez-Miragall & Martinez-Salas, 2003). This motif was modified in the cDNA to either GAGA or GTTA, as such mutants in the EMCV IRES have less than 10% of wt IRES activity (Robertson *et al.*, 1999).

*Reduced level of 3C$^{pro}$ activity enhances accumulation of processed FMDV capsid proteins*

In the following experiments, plasmids which produce monocistronic (P1-2A and P1-2A-3C) and dicistronic RNA transcripts (P1-2A-mIRES-3C) from the T7 promoter were transfected into BHK cells infected with the vaccinia virus vTF7-3, which expresses the T7 RNA polymerase (Fuerst *et al.*, 1986). After 20 h, cytosolic extracts were prepared and analysed for the presence of FMDV capsid proteins, 3C$^{pro}$ and β-actin by immunoblotting. As expected, no FMDV proteins were detected by the antisera in the absence of any transfected plasmid (Fig. 2a, b, lanes 1). In the absence of 3C$^{pro}$, the unprocessed P1-2A precursor was produced from both the serotype O and A cDNA cassettes (approx. 85 kDa, Fig. 2a, b, lanes 2) as observed previously (Polacek *et al.*, 2013). When the 3C$^{pro}$ sequence was included in the cassettes then processing of the P1-2A occurred, but the extent of processing observed and the accumulation of the processed products varied with the level of 3C$^{pro}$ activity that was expressed (see Fig. 2). The use of wt 3C$^{pro}$ resulted in near complete processing of P1-2A (see Fig. 2a, b, lanes 3, 5 and 6) into the individual capsid proteins VP0 (approx. 36 kDa) and VP1 (approx. 28 kDa) in accordance with the expected sizes (33 kDa and 23 kDa, respectively, Fig. 2, lanes 3 to 10). Note, the VP3 capsid protein (approx. 24 kDa) was not efficiently recognized by this polyclonal anti-FMDV antibody (M.G., C.P. & G.J.B., unpublished results). For both serotypes O and A, the P1-2A-3CC142S constructs (with a mutant 3C$^{pro}$) yielded increased levels of the processed capsid proteins compared to the P1-2A-3Cwt constructs (Fig. 2a, b, compare lanes 3 and 4). Using serotype O cassettes, a VP1/VP1-2A doublet was observed (Fig. 2a; these products were identified using P1 and P1-2A FMDV cDNA

cassettes, M.G., C.P. & G.J.B., unpublished results). A higher level accumulation of the $3C^{pro}$ (C142S) mutant compared to the wt $3C^{pro}$ was detected by immunoblotting (Fig. 2), as observed previously in co-transfection experiments (Polacek *et al*., 2013). This is likely due to the fact that the $3C^{pro}$ C142S mutant does not inhibit its own synthesis (see Discussion). Amongst all of the different constructs and independent of serotype, the P1-2A-mIRES-3C cassettes containing the GTTA mIRES element with reduced IRES activity together with the wt $3C^{pro}$ produced the highest amounts of processed capsid proteins (Fig. 2a, b, lanes 7). In contrast, no increased capsid protein accumulation was observed for the construct containing the GAGA mutant compared to the wt IRES (Fig. 2a, b, compare lanes 5 and 6). As expected, the mIRES element with the tetraloop sequence GTTA, in combination with the $3C^{pro}$ C142S, reduced the $3C^{pro}$ enzyme activity to lower levels compared to the combination with 3Cwt. Proteolytic activity was still observed, but higher levels of unprocessed P1-2A precursor and intermediates, i.e. VP0-VP3 and VP3-VP1, were detected (Fig. 2a, b, compare lanes 7 and 10). The accumulation of $3C^{pro}$ itself was detected by immunoblotting from all the FMDV cDNA cassettes containing the coding sequence for $3C^{pro}$ (as expected) except for the P1-2A-IRESgtta3Cwt and P1-2A-IRESgtta3CC142S (see Fig. 2a, b, lanes 7 and 10). Taken together, the results showed that co-expression of the P1-2A precursor with the 3C C142S mutant, or use of the defective mIRES element (containing the GTTA motif) with the wt $3C^{pro}$, produced the highest level of the processed FMDV capsid proteins.

*Binding of the FMDV capsid proteins to serotype-specific anti-FMDV antibodies and to the integrin $\alpha_v\beta_6$*

We have shown previously (Polacek *et al*. 2013), that the P1-2A capsid precursor proteins, and the $3C^{pro}$-processed products, are recognized in serotype-specific enzyme-linked

191 immunosorbent assays (ELISAs) which were used to determine their antigenicity and also bind to
192 the major cellular receptor for FMDV, $\alpha_v\beta_6$ integrin (Ferris *et al*., 2005). The expressed FMDV
193 capsid proteins as analysed in Fig. 2, were also tested using these ELISAs (Fig. 3). As expected,
194 the FMDV proteins bound to both serotype-specific anti-FMDV antibodies and to the $\alpha_v\beta_6$
195 integrin. Furthermore, considering these results together with the immunoblot analysis of protein
196 expression, it was concluded that the optimal production of processed FMDV capsid proteins was
197 achieved when the P1-2A precursor (of both serotypes) was expressed with low levels of $3C^{pro}$
198 activity within the P1-2A-IRESgtta3Cwt cassettes (Fig. 2 and Fig. 3).
199
200 *Self-assembly of processed capsid proteins into empty FMDV-like particles*
201 To verify that the processed capsid proteins self-assembled into FMDV empty capsid particles
202 (75S), cell lysates were analysed by sucrose gradient ultracentrifugation and the fractions were
203 examined using the serotype-specific antigen ELISAs. Protomers (5S) were detected near the top
204 of the gradient (fractions 2-4, Fig. 4a, b) and empty capsid particles were detected near the
205 bottom of the gradient (fractions 13-15, Fig. 4a, b). Consistent with the results described above,
206 expression of high amounts of $3C^{pro}$ was not beneficial for FMDV capsid assembly. The yield of
207 empty capsid particles from the P1-2A-3Cwt plasmid was low but was increased with a mutant
208 $3C^{pro}$ (P1-2A-3CC142S) and the highest level of assembled capsids was generated from the P1-
209 2A-IRESgtta3Cwt plasmid. Western blot analysis of the empty capsid fractions from the sucrose
210 gradients showed that they contained the expected structural proteins VP0 and VP1, while no
211 intact P1-2A precursor protein was present (Fig. 4c, d). However, significant breakdown of the
212 VP0 within the empty capsid fractions was detected using a VP2-specific antibody and the
213 product matched the expected size for authentic processing of VP0 (approx. 33 kDa) into VP2
214 (approx. 24 kDa) and VP4 (approx. 9 kDa, not detectable with this gel system).

*Empty FMDV-like capsid particles bind to the $\alpha_v\beta_6$ integrin receptor*

To characterize the properties of the protomers and assembled empty capsids (from both serotype O and A), these products were examined, directly after sucrose gradient purification, for their ability to bind to $\alpha_v\beta_6$ integrin in the presence or absence of EDTA. These assays showed that both the protomers and the assembled empty capsids can bind, in a divalent cation dependent manner, to the purified RGD-dependent integrin $\alpha_v\beta_6$ (Fig. 5a, b) as observed with the whole virus (Jackson *et al.*, 2000).

To extend and support the results described above, we further analysed the purified serotype O and A empty capsids in the serotype-specific ELISAs and in the $\alpha_v\beta_6$ integrin binding assay (Fig. 5c, d). As expected, no cross-reactions were observed between the empty capsid particles from the two different serotypes using the serotype-specific antigen ELISAs (Fig. 5c). Furthermore, the detection of serotype A empty capsids bound to $\alpha_v\beta_6$ integrin was also serotype specific (Fig. 5d). In contrast, in the ELISA using a guinea pig anti-type O FMDV antiserum, both the serotype O and A antigens, when bound to $\alpha_v\beta_6$ integrin, were detected with equal efficiency (Fig. 5d). Thus, one-way, cross-reactivity was observed with the assembled empty capsids in this assay.

*Morphological similarities between purified FMDV serotype A empty capsids and the virus*

To determine the size and the morphology of the assembled empty capsids, sucrose gradient-purified FMDV serotype A empty particles were examined by transmission electron microscopy and the images were used for three-dimensional reconstruction. Negatively stained purified empty FMDV particles appeared as uniform spherical empty virion-like particles with a densely stained core and a median size of approx. 30 nm in diameter (Fig. 6a). In total, 138 empty capsid particles were used for the three-dimensional reconstruction with a final resolution of 36Å (Fig.

6b). The reconstruction had a less defined surface compared to the low-resolution (8Å) model calculated from the X-ray crystal structure of FMDV serotype A1061 (Fig. 6c) (Fry *et al.*, 2005). However, the overall surface-appearance of the reconstructed empty capsid particle was ordered and repetitive, and resembled FMDV morphologically with distinct five-fold, three-fold and two-fold axes of symmetry. The elevation of certain features on the particle surface appeared different from the structure determined for the virus by crystallography. Attempts to study purified FMDV serotype O empty capsids were not successful, due to stability issues.

**Discussion**

In this study, we have analysed different strategies to determine the optimal system for the production, processing and assembly of FMDV capsid proteins within mammalian cells by the efficient expression of the structural protein precursor (P1-2A) together with a limited amount of the $3C^{pro}$ that is sufficient to achieve P1-2A processing but without adverse effects on the expression system. Recently, Porta *et al.*, (2013a) showed that a low level of $3C^{pro}$ activity can be sufficient to achieve FMDV P1-2A processing in insect cell systems. Similarly, it has been demonstrated that co-transfection of a plasmid encoding P1-2A with low levels of a second plasmid encoding $3C^{pro}$ was sufficient to achieve efficient processing of the P1-2A to the mature FMDV empty capsid proteins within mammalian cells (Polacek *et al*., 2013). The studies presented here have now extended these observations using a mIRES-containing dicistronic mRNA expression system to achieve a low level of $3C^{pro}$ expression relative to the P1-2A. The cDNA sequences encoding the capsid protein precursor (P1-2A) and $3C^{pro}$, with a mutant IRES located between them, were expressed from a dicistronic mRNA. Production of $3C^{pro}$ was dependent on a modified FMDV IRES, with a  mutation in the GNRA motif (GCGA to GTTA) known to inhibit the EMCV IRES element (Robertson *et al.*, 1999). Using this system it was

possible to achieve the highest expression and processing of the mature empty capsid components, i.e. VP0, VP1 and VP3. Furthermore, these proteins self-assembled into empty capsid particles (or virus-like particles), as determined by sucrose gradient analyses and electron microscopy. The strategy was reproducible since very similar results were obtained for the two most common serotypes, namely O and A.

It is noteworthy that the GAGA tetraloop mIRES, previously shown to decrease the efficiency of the EMCV IRES (Robertson *et al.*, 1999), was as active as the wt FMDV IRES element even though the FMDV IRES is predicted to have a secondary structure that is closely related to the EMCV IRES (Pilipenko *et al.*, 1989). The precise role of the GNRA tetraloop in IRES function is unknown; no protein interactions have been localised to this site, but it is believed to be important for RNA-RNA interactions required to maintain the IRES tertiary structure (Fernandez-Miragall *et al.*, 2009).

As an alternative strategy for expressing a reduced level of $3C^{pro}$ activity, a monocistronic expression vector with the FMDV capsid protein precursor linked to the $3C^{pro}$ C142S mutant (Sweeney *et al.*, 2007) was also evaluated. The results indicated that the $3C^{pro}$ mutant does not limit its own expression as effectively as the $3C^{pro}$ wt (as may be expected due to its lower catalytic activity) and hence the level of mutant $3C^{pro}$ protein expression was higher compared to the $3C^{pro}$ wt (Fig. 2a, b). These results are consistent with the fact that $3C^{pro}$ not only cleaves the viral precursor proteins, but also a variety of cellular substrates associated with translation (Belsham *et al.*, 2000) and transcription (Falk *et al.*, 1990).

Proteolytic processing of the VP0 precursor into VP4 and VP2 is required for virion maturation and infectivity but the mechanism of cleavage is unknown (Ansardi *et al.*, 1992; Moscufo *et al.*, 1991). Previously, it was believed that RNA encapsidation was essential to trigger the cleavage of VP0, but Curry *et al.* (1995) demonstrated that a fairly slow cleavage of

287 VP0 in FMDV does not require the presence of RNA. Under the experimental conditions
288 described, the results presented in Fig. 4 (c, d), using an anti-FMDV VP2 antibody, indicated that
289 a large proportion of the VP0 precursor protein in the purified empty capsid particles had been
290 processed (as indicated by the formation of VP2).

291 The empty FMDV particles displayed the $\alpha_v\beta_6$ integrin binding activity of the native virion, as
292 demonstrated by ELISAs (Fig. 5). As expected (Dicara *et al.*, 2008; Goodwin *et al.*, 2009), the
293 $Ca^{2+}$ dependent binding of FMDV capsid proteins to $\alpha_v\beta_6$ integrin was completely inhibited by 10
294 mM EDTA, a strong inhibitor of divalent cation-dependent integrin-ligand interaction. The
295 results from the serotype-specific ELISAs also indicated that the assembled capsids possess
296 antigenicity similar to that of FMDV virus particles and are therefore capable of serving as
297 antigens to detect FMDV-specific antibodies. However, the serotype-specificity of the assay
298 relies on the use of two separate antisera for the capture and detection of the antigen and when
299 the type O antigen was captured using the integrin then the guinea pig anti-FMDV antibodies
300 failed to distinguish between serotype O and serotype A.

301 The characteristics of the empty capsid particles suggested that these FMDV empty capsid
302 particles may have a similar tertiary structure as the virus. Indeed, when the self-assembled
303 empty capsid particles were examined by electron microscopy and three-dimensional
304 reconstruction, the serotype A empty capsid particles were found to closely resemble FMDV
305 viruses in size and overall particle morphology (but see below). We did not succeed in observing
306 the serotype O empty capsid particles using electron microscopy due to stability issues. It has
307 been noted previously that serotype A particles are more robust than serotype O particles
308 (Abrams *et al.*, 1995; Porta *et al.*, 2013a). Lack of assembled empty capsid proteins might
309 explain why a candidate vaccine based on a replication-deficient adenovirus vector containing the

capsid coding region of serotype O and the $3C^{pro}$ induced less effective protection than the equivalent serotype A system (Moraes *et al.*, 2002; Moraes *et al.*, 2011; Pacheco *et al.*, 2005).

Previous comparisons of the crystal structures of virions and natural empty capsids of FMDV A (Curry *et al.*, 1996; Curry *et al.*, 1997; Fry *et al.*, 2005) revealed identical packaging of the capsid proteins in both particles. The virions have a more ordered structure than the empty capsid particles in the region of the three-fold axes of symmetry and the observed differences, on the interior surface of the capsid, were correlated with the presence of the RNA. In the reconstructions of the expressed empty capsid particles obtained using electron microscopy which are presented here, the elevation of different features of the particle surface seems distinct from that observed in the crystal structures (see Fig. 6b, c). The low resolution three-dimensional reconstruction exaggerates some of the surface features visible on the map simulated from the crystal structure. Namely the pore-like depression at the five-fold vertex and the elevated three-fold plateaus are more pronounced. However, this may be due to lack of detail from the limited resolution or an effect of particles being coated with heavy metal stain in the rather harsh process. Thus we cannot rigorously compare them as they are not of equal quality but we can rely on the low resolution result to be largely accurate overall. This methodology, based on analytical scale production of the empty capsids using a transient expression system, may be suitable for screening the effect of modifications to the virus proteins on capsid assembly.

The optimized co-expression of FMDV proteins, using the P1-2A-mIRES-3C cassettes, should serve as a platform for the improved production of FMDV empty capsids using a virus vector system and contribute to the development of improved and safer next generation FMD vaccines and the production of non-infectious diagnostic reagents. These systems should also facilitate future studies on capsid assembly, circumventing the handling of large amounts of infectious virus.

## Methods

### Plasmid constructions

The FMDV cDNA cassettes used are shown in Fig. 1. The plasmids were prepared by standard methods (Sambrook *et al.*, 1989) and primers used are listed in Supplementary Table 1. The cDNA sequences corresponding to the O1 Manisa FMDV (pGEM-3Z-O-P1-2A) and the A22 FMDV (pGEM-3Z-A-P1-2A) capsid precursors have been described (Polacek *et al.*, 2013; Porta *et al.*, 2013a). The IRES element from FMDV O1K cDNA (as in pT7S3, Ellard *et al.*, 1999) was amplified with a T7 primer and a primer (IRES_*Sac*I*Bam*HI_Re) flanked by a *Sac*I-*Bam*HI sites using, as template, a monocistronic reporter plasmid, pFMDRluc (G.J.B., unpublished, derived from pRBRluc, Belsham *et al.*, 2008). This IRES wild type (wt) segment was digested with *Eco*RI and *Bam*HI and ligated into similarly digested pGEM-3Z (Promega) to produce pGEM-3Z-IRESwt. To construct the two IRES mutants, the wt GNRA tetraloop sequence GCGA was converted to GAGA or GTTA (Robertson *et al.*, 1999) using primers containing a *Sty*I site (IRES_gtta_*Sty*I_Fw or IRES_gaga_*Sty*I_Fw) and the reverse primer (IRES_*Sac*I*Bam*HI_Re) as above. The amplified fragments were digested with *Sty*I and *Bam*HI and ligated into the same sites of pGEM-3Z-IRESwt to create pGEM-3Z-IRESgaga and pGEM-3Z-IRESgtta, respectively. The plasmids encoding the wt FMDV $3C^{pro}$ and a modified $3C^{pro}$ with reduced protease activity (C95K and C142S) (Birtley *et al.*, 2005; Sweeney *et al.*, 2007), were kindly provided by S. Curry, Imperial College, United Kingdom. The 3Cwt or 3CC142S cDNA sequences were amplified with primers flanked by *Sac*I and *Bam*HI sites (3C_*Sac*I_Fw and 3C_*Xma*I*Bam*HI_Re), digested and ligated into the same sites of the pGEM-3Z-IRES vectors containing IRESwt, IRESgaga or IRESgtta. The 3Cwt, 3CC142S and IRES3C fragments were amplified using the 3C or IRES3C plasmids as templates and primers containing an *Asc*I site (3C_*Asc*I_Fw or IRES_*Asc*I_Fw and 3C_*Asc*I_Re). The PCR products were digested with *Asc*I

and then ligated into the *Asc*I-digested backbone of pGEM-3Z-P1-2A to produce the expression plasmids pGEM-3Z-P1-2A-3Cwt (Polacek *et al.*, 2013), pGEM-3Z-P1-2A-3CC142S and the six different combinations of pGEM-3Z-P1-2A-IRES3C (IRESwt3Cwt, IRESgaga3Cwt, IRESgtta3Cwt, IRESwt3CC142S, IRESgaga3CC142S and IRESgtta3CC142S) (see Fig. 1). All constructs were propagated in *Escherichia coli* Top10 cells (Invitrogen), purified (Midiprep kit, Fermentas) and verified by sequencing.

**Transient-expression assays**

Monolayers (35 mm wells) of baby hamster kidney (BHK) cells (90% confluent) were infected with vTF7-3, a recombinant vaccinia virus that expresses T7 RNA polymerase (Fuerst *et al.*, 1986) as described previously (Belsham *et al.*, 2008). Cell lysates were prepared 20 h post transfection with 20 mM Tris-HCl (pH 8.0), 125 mM NaCl and 0.5% NP-40 and clarified by centrifugation at 18,000xg for 10 min at 4°C.

**Western blot analysis**

Samples were mixed with Laemmli sample buffer, resolved by sodium dodecyl sulfate polyacrylamide gel electrophoresis (SDS-PAGE, 12.5% or 15% polyacrylamide) and electroblotted onto polyvinylidene difluoride membranes (Millipore) as described previously (Polacek *et al.*, 2013). The following primary antibodies were used: anti-FMDV O1 Manisa serum, anti-FMDV 3C 1G1 (kindly provided by E. Brocchi, Brescia, Italy, as used previously, Belsham *et al.*, 2000), serotype-independent anti-FMDV VP2 4B2 (kindly provided by L. Yu, Harbin, China, Yu *et al.*, 2011), and anti-actin (ab8227, Abcam). Immunoreactive proteins were visualized using species-specific anti-Ig secondary antibodies conjugated to horseradish

peroxidase (P0448, P0141 and P0161, Dako) with a ECL Prime detection system (Amersham) on a Bio-Rad Chemi-Doc XRS system.

**ELISAs**

Serotype-specific FMDV antigen ELISAs, for serotype O and A as appropriate, were performed as described previously (OIE, 2008; Roeder & Le Blanc Smith, 1987; Polacek *et al.*, 2013) and the absorbance was read at 450 nm and 620 nm. The ELISA assay to detect FMDV antigen binding to the integrin receptor $\alpha_v\beta_6$ was performed essentially as described (Ferris *et al.*, 2005; Ferris *et al.*, 2011), with some minor modifications (Polacek *et al.*, 2013). Non-specific binding was determined in the presence of 10 mM EDTA. Detection of the bound FMDV antigen was achieved using guinea pig anti-FMDV polyclonal serum as for the serotype-specific FMDV antigen ELISAs.

**Sucrose gradient centrifugation**

Cell extracts (400 µl from one 35 mm well per gradient) were loaded onto gradients of 10 to 30% (w/v) sucrose in 40 mM sodium phosphate buffer (pH 7.6), 100 mM NaCl (buffer P) and centrifuged at 245,000xg in a SW 55 Ti rotor (Beckman Coulter) for 2.5 h at 10°C. Fractions were collected from the top of the gradient and viral proteins were detected by serotype-specific ELISAs (as above). To obtain assembled empty FMDV capsids, the particles were separated from the cell lysates (three 6-well plates) by centrifugation through a 30% sucrose cushion (w/v) in buffer P at 245,000xg for 2 h at 10°C. The pellet was dissolved in buffer P and treated with 0.1 mg $ml^{-1}$ RNase A for 5 min before fractionation on a sucrose gradient as described above. Fractions containing empty capsids were concentrated using an Amicon Ultra 100 kDa centrifuge filter device (Millipore).

## Electron microscopy and reconstruction

An aliquot of 3 µl of sucrose gradient purified FMDV serotype A empty capsids was placed on a freshly glow-discharged continuous carbon-coated copper grid. NanoVan stain (Nanoprobes, Yaphank, NY) was applied by the standard drop method, and the sample was examined in a JEOL 1400 transmission electron microscope at 120 kV. For the three-dimensional reconstruction, 40 CCD micrographs were recorded with a Gatan Orius SC 1000 camera with Digital Micrograph at a calibrated magnification of 33,090x. In total, 138 particles were selected using RobEM (Yan *et al.*, 2007) and 127 were used for the reconstruction. The defocus distance ranged from 0.67 to 2.08 µm. The final pixel size was 2.72Å. The reconstruction processes were performed using icosahedral averaging with the program AUTO3DEM, which generated a random model directly from the raw data as the initial starting structure (Yan *et al.*, 2007). The final resolution of 36Å was determined from where the Fourier shell correlation fell below 0.5. The final reconstruction was colored radially using the program Chimera (Pettersen *et al.*, 2004). The 8Å calculated map was made using the X-ray crystallography structure of FMDV A1061 from the Protein Data Bank file, accession number 1ZBE (Fry *et al.*, 2005), using the Situs program pdb2vol (Wriggers, 2010).


## Acknowledgments

We wish to thank Emiliana Brocchi (IZSLER, Italy) for providing the anti-3C antibodies, Stephen Curry (Imperial College, United Kingdom) for the $3C^{pro}$ plasmids and Li Yu (The Chinese Academy of Agricultural Sciences, China) for the anti-VP2 antibody. We would also like to acknowledge the excellent technical assistance from Tina Rasmussen, Preben Normann and Inge Nielsen at Lindholm.

428 This work was supported by the Danish Council for Independent Research | Technology and
429 Production Sciences (FTP grants 09-070549 (to C.P.) and 274-07-0104 (to G.J.B)), the Helge
430 Ax:son Johnsons Foundation and the Microscope Imaging Core Facility at the Pennsylvania State
431 University College of Medicine.

## References

**Abrams, C. C., King, A. M. & Belsham, G. J. (1995).** Assembly of foot-and-mouth disease virus empty capsids synthesized by a vaccinia virus expression system. *J Gen Virol* **76**, 3089-3098.

**Acharya, R., Fry, E., Stuart, D., Fox, G., Rowlands, D. & Brown, F. (1989).** The three-dimensional structure of foot-and-mouth disease virus at 2.9 A resolution. *Nature* **337**, 709-716.

**Alexandersen, S., Zhang, Z., Donaldson, A. I. & Garland, A. J. (2003).** The pathogenesis and diagnosis of foot-and-mouth disease. *J Comp Pathol* **129**, 1-36.

**Ansardi, D. C., Porter, D. C. & Morrow, C. D. (1992).** Myristylation of poliovirus capsid precursor P1 is required for assembly of subviral particles. *J Virol* **66**, 4556-4563.

**Armer, H., Moffat, K., Wileman, T., Belsham, G. J., Jackson, T., Duprex, W. P., Ryan, M. & Monaghan, P. (2008).** Foot-and-mouth disease virus, but not bovine enterovirus, targets the host cell cytoskeleton via the nonstructural protein 3Cpro. *J Virol* **82**, 10556-10566.

**Belsham, G. J. (2005).** Translation and replication of FMDV RNA. *Curr Top Microbiol Immunol* **288**, 43-70.

**Belsham, G. J., McInerney, G. M. & Ross-Smith, N. (2000).** Foot-and-mouth disease virus 3C protease induces cleavage of translation initiation factors eIF4A and eIF4G within infected cells. *J Virol* **74**, 272-280.

**Belsham, G. J., Nielsen, I., Normann, P., Royall, E. & Roberts, L. O. (2008).** Monocistronic mRNAs containing defective hepatitis C virus-like picornavirus internal ribosome entry site elements in their 5' untranslated regions are efficiently translated in cells by a cap-dependent mechanism. *RNA* **14**, 1671-1680.

**Birtley, J. R., Knox, S. R., Jaulent, A. M., Brick, P., Leatherbarrow, R. J. & Curry, S. (2005).** Crystal structure of foot-and-mouth disease virus 3C protease. New insights into catalytic mechanism and cleavage specificity. *J Biol Chem* **280**, 11520-11527.

**Bøtner, A., Kakker, N. K., Barbezange, C., Berryman, S., Jackson, T. & Belsham, G. J. (2011).** Capsid proteins from field strains of foot-and-mouth disease virus confer a pathogenic phenotype in cattle on an attenuated, cell-culture-adapted virus, O1 Kaufbeuren virus. *J Gen Virol* **92**, 1141-1151.

**Bouma, A., Elbers, A. R., Dekker, A., de Koeijer, A., Bartels, C., Vellema, P., van der Wal, P., van Rooij, E. M., Pluimers, F. H. & de Jong, M. C. (2003).** The foot-and-mouth disease epidemic in The Netherlands in 2001. *Prev Vet Med* **57**, 155-166.

**Cao, Y., Lu, Z., Sun, J., Bai, X., Sun, P., Bao, H., Chen, Y., Guo, J., Li, D., Liu, X. & Liu, Z. (2009).** Synthesis of empty capsid-like particles of Asia I foot-and-mouth disease virus in insect cells and their immunogenicity in guinea pigs. *Vet Microbiol* **137**, 10-17.

**Chow, M., Newman, J. F., Filman, D., Hogle, J. M., Rowlands, D. J. & Brown, F. (1987).** Myristylation of picornavirus capsid protein VP4 and its structural significance. *Nature* **327**, 482-486.

**Chung, C. Y., Chen, C. Y., Lin, S. Y., Chung, Y. C., Chiu, H. Y., Chi, W. K., Lin, Y. L., Chiang, B. L., Chen, W. J. & Hu, Y. C. (2010).** Enterovirus 71 virus-like particle vaccine: improved production conditions for enhanced yield. *Vaccine* **28**, 6951-6957.

**Curry, S., Abrams, C. C., Fry, E., Crowther, J. C., Belsham, G. J., Stuart, D. I. & King, A. M. (1995).** Viral RNA modulates the acid sensitivity of foot-and-mouth disease virus capsids. *J Virol* **69**, 430-438.

**Curry, S., Fry, E., Blakemore, W., Abu-Ghazaleh, R., Jackson, T., King, A., Lea, S., Newman, J., Rowlands, D. & Stuart, D. (1996).** Perturbations in the surface structure of A22

Iraq foot-and-mouth disease virus accompanying coupled changes in host cell specificity and antigenicity. *Structure* **4**, 135-145.

**Curry, S., Fry, E., Blakemore, W., Abu-Ghazaleh, R., Jackson, T., King, A., Lea, S., Newman, J. & Stuart, D. (1997).** Dissecting the roles of VP0 cleavage and RNA packaging in picornavirus capsid stabilization: the structure of empty capsids of foot-and-mouth disease virus. *J Virol* **71**, 9743-9752.

**Dicara, D., Burman, A., Clark, S., Berryman, S., Howard, M. J., Hart, I. R., Marshall, J. F. & Jackson, T. (2008).** Foot-and-mouth disease virus forms a highly stable, EDTA-resistant complex with its principal receptor, integrin alphavbeta6: implications for infectiousness. *J Virol* **82**, 1537-1546.

**Ellard, F. M., Drew, J., Blakemore, W. E., Stuart, D. I. & King, A. M. (1999).** Evidence for the role of His-142 of protein 1C in the acid-induced disassembly of foot-and-mouth disease virus capsids. *J Gen Virol* **80**, 1911-1918.

**Falk, M. M., Grigera, P. R., Bergmann, I. E., Zibert, A., Multhaup, G. & Beck, E. (1990).** Foot-and-mouth disease virus protease 3C induces specific proteolytic cleavage of host cell histone H3. *J Virol* **64**, 748-756.

**Fernandez-Miragall, O., Lopez de Quinto, S. & Martinez-Salas, E. (2009).** Relevance of RNA structure for the activity of picornavirus IRES elements. *Virus Res* **139**, 172-182.

**Fernandez-Miragall, O. & Martinez-Salas, E. (2003).** Structural organization of a viral IRES depends on the integrity of the GNRA motif. *RNA* **9**, 1333-1344.

**Ferris, N. P., Abrescia, N. G., Stuart, D. I., Jackson, T., Burman, A., King, D. P. & Paton, D. J. (2005).** Utility of recombinant integrin alpha v beta6 as a capture reagent in immunoassays for the diagnosis of foot-and-mouth disease. *J Virol Methods* **127**, 69-79.

**Ferris, N. P., Grazioli, S., Hutchings, G. H. & Brocchi, E. (2011).** Validation of a recombinant integrin alphavbeta6/monoclonal antibody based antigen ELISA for the diagnosis of foot-and-mouth disease. *J Virol Methods* **175**, 253-260.

**Fry, E. E., Newman, J. W., Curry, S., Najjam, S., Jackson, T., Blakemore, W., Lea, S. M., Miller, L., Burman, A., King, A. M. & Stuart, D. I. (2005).** Structure of Foot-and-mouth disease virus serotype A10 61 alone and complexed with oligosaccharide receptor: receptor conservation in the face of antigenic variation. *J Gen Virol* **86**, 1909-1920.

**Fuerst, T. R., Niles, E. G., Studier, F. W. & Moss, B. (1986).** Eukaryotic transient-expression system based on recombinant vaccinia virus that synthesizes bacteriophage T7 RNA polymerase. *Proc Natl Acad Sci U S A* **83**, 8122-8126.

**Goodwin, S., Tuthill, T. J., Arias, A., Killington, R. A. & Rowlands, D. J. (2009).** Foot-and-mouth disease virus assembly: processing of recombinant capsid precursor by exogenous protease induces self-assembly of pentamers in vitro in a myristoylation-dependent manner. *J Virol* **83**, 11275-11282.

**Grubman, M. J. & Baxt, B. (2004).** Foot-and-mouth disease. *Clin Microbiol Rev* **17**, 465-493.

**Jackson, T., Ellard, F. M., Ghazaleh, R. A., Brookes, S. M., Blakemore, W. E., Corteyn, A. H., Stuart, D. I., Newman, J. W. & King, A. M. (1996).** Efficient infection of cells in culture by type O foot-and-mouth disease virus requires binding to cell surface heparan sulfate. *J Virol* **70**, 5282-5287.

**Jackson, T., Sheppard, D., Denyer, M., Blakemore, W. & King, A. M. (2000).** The epithelial integrin alphavbeta6 is a receptor for foot-and-mouth disease virus. *J Virol* **74**, 4949-4956.

**Lohse, L., Jackson, T., Bøtner, A. & Belsham, G. J. (2012).** Capsid coding sequences of foot-and-mouth disease viruses are determinants of pathogenicity in pigs. *Vet Res* **43**, 46.

**Lopez de Quinto, S. & Martinez-Salas, E. (1997).** Conserved structural motifs located in distal loops of aphthovirus internal ribosome entry site domain 3 are required for internal initiation of translation. *J Virol* **71**, 4171-4175.

**Martinez-Salas, E. & Domingo, E. (1995).** Effect of expression of the aphthovirus protease 3C on viral infection and gene expression. *Virology* **212**, 111-120.

**Medina, M., Domingo, E., Brangwyn, J. K. & Belsham, G. J. (1993).** The two species of the foot-and-mouth disease virus leader protein, expressed individually, exhibit the same activities. *Virology* **194**, 355-359.

**Monaghan, P., Gold, S., Simpson, J., Zhang, Z., Weinreb, P. H., Violette, S. M., Alexandersen, S. & Jackson, T. (2005).** The alpha(v)beta6 integrin receptor for Foot-and-mouth disease virus is expressed constitutively on the epithelial cells targeted in cattle. *J Gen Virol* **86**, 2769-2780.

**Moraes, M. P., Mayr, G. A., Mason, P. W. & Grubman, M. J. (2002).** Early protection against homologous challenge after a single dose of replication-defective human adenovirus type 5 expressing capsid proteins of foot-and-mouth disease virus (FMDV) strain A24. *Vaccine* **20**, 1631-1639.

**Moraes, M. P., Segundo, F. D., Dias, C. C., Pena, L. & Grubman, M. J. (2011).** Increased efficacy of an adenovirus-vectored foot-and-mouth disease capsid subunit vaccine expressing nonstructural protein 2B is associated with a specific T cell response. *Vaccine* **29**, 9431-9440.

**Moscufo, N., Simons, J. & Chow, M. (1991).** Myristoylation is important at multiple stages in poliovirus assembly. *J Virol* **65**, 2372-2380.

**OIE (2008).** Foot-and-mouth disease. Manual of standards for diagnostic test and vaccines for terrestrial animals. http://web.oie.int/eng/normes/MMANUAL/2008/pdf/2.01.05_FMD.pdf

**Pacheco, J. M., Brum, M. C., Moraes, M. P., Golde, W. T. & Grubman, M. J. (2005).** Rapid protection of cattle from direct challenge with foot-and-mouth disease virus (FMDV) by a single inoculation with an adenovirus-vectored FMDV subunit vaccine. *Virology* **337**, 205-209.

**Pettersen, E. F., Goddard, T. D., Huang, C. C., Couch, G. S., Greenblatt, D. M., Meng, E. C. & Ferrin, T. E. (2004).** UCSF Chimera--a visualization system for exploratory research and analysis. *J Comput Chem* **25**, 1605-1612.

**Pilipenko, E. V., Blinov, V. M., Chernov, B. K., Dmitrieva, T. M. & Agol, V. I. (1989).** Conservation of the secondary structure elements of the 5'-untranslated region of cardio- and aphthovirus RNAs. *Nucleic Acids Res* **17**, 5701-5711.

**Polacek, C., Gullberg, M., Li, J. & Belsham, G. J. (2013).** Low levels of foot-and-mouth disease virus $3C^{pro}$ expression are required to achieve optimal capsid protein expression and processing in mammalian cells. *J. Gen. Virol.* **94** (in press) Published online ahead of print doi: 10.1099/vir.0.050492-0

**Porta, C., Xu, X., Loureiro, S., Paramasivam, S., Ren, J., Al-Khalil, T., Burman, A., Jackson, T., Belsham, G. J., Curry, S., Lomonossoff, G. P., Parida, S., Paton, D., Li, Y., Wilsden, G., Ferris, N., Owens, R., Kotecha, A., Fry, E., Stuart, D. I., Charleston, B. & Jones, I. M. (2013a).** Efficient production of foot-and-mouth disease virus empty capsids in insect cells following down regulation of 3C protease activity. *J Virol Methods* **187**, 406-412.

**Porta, C., Kotecha, A., Burman, A., Jackson, T., Ren, J., Loureiro, S., Jones, I.M., Fry, E.E., Stuart, D.I. & Charleston, B. (2013b).** Rational engineering of recombinant picornavirus capsids to produce safe, protective vaccine antigen. PLoS Pathog. 9(3):e1003255. doi: 10.1371/journal.ppat.1003255.

**Roberts, L. O. & Belsham, G. J. (1997).** Complementation of defective picornavirus internal ribosome entry site (IRES) elements by the coexpression of fragments of the IRES. *Virology* **227**, 53-62.

**Robertson, M. E., Seamons, R. A. & Belsham, G. J. (1999).** A selection system for functional internal ribosome entry site (IRES) elements: analysis of the requirement for a conserved GNRA tetraloop in the encephalomyocarditis virus IRES. *RNA* **5,** 1167-1179.

**Rodriguez, L. L. & Grubman, M. J. (2009).** Foot and mouth disease virus vaccines. *Vaccine* **27** Suppl 4, D90-94.

**Roeder, P. L. & Le Blanc Smith, P. M. (1987).** Detection and typing of foot-and-mouth disease virus by enzyme-linked immunosorbent assay: a sensitive, rapid and reliable technique for primary diagnosis. *Res Vet Sci* **43**, 225-232.

**Rowlands, D. J., Sangar, D. V. & Brown, F. (1975).** A comparative chemical and serological study of the full and empty particles of foot-and mouth disease virus. *J Gen Virol* **26**, 227-238.

**Sa-Carvalho, D., Rieder, E., Baxt, B., Rodarte, R., Tanuri, A. & Mason, P. W. (1997).** Tissue culture adaptation of foot-and-mouth disease virus selects viruses that bind to heparin and are attenuated in cattle. *J Virol* **71**, 5115-5123.

**Saiz, J. C., Cairo, J., Medina, M., Zuidema, D., Abrams, C., Belsham, G. J., Domingo, E. & Vlak, J. M. (1994).** Unprocessed foot-and-mouth disease virus capsid precursor displays discontinuous epitopes involved in viral neutralization. *J Virol* **68**, 4557-4564.

**Sambrook, J., Fritsch, E. F. & Maniatis, T. (1989).** *Molecular cloning: a laboratory manual* Cold Spring Harbor NY Cold Spring Harbor Laboratory.

**Sweeney, T. R., Roque-Rosell, N., Birtley, J. R., Leatherbarrow, R. J. & Curry, S. (2007).** Structural and mutagenic analysis of foot-and-mouth disease virus 3C protease reveals the role of the beta-ribbon in proteolysis. *J Virol* **81**, 115-124.

**Wriggers, W. (2010).** Using Situs for the integration of multi-resolution structures. *Biophys Rev* **2**, 21-27.

**Yan, X., Sinkovits, R. S. & Baker, T. S. (2007).** AUTO3DEM--an automated and high throughput program for image reconstruction of icosahedral particles. *J Struct Biol* **157**, 73-82.

**Yu, Y., Wang, H., Zhao, L., Zhang, C., Jiang, Z. & Yu, L. (2011).** Fine mapping of a foot-and-mouth disease virus epitope recognized by serotype-independent monoclonal antibody 4B2. *J Microbiol* **49**, 94-101.

## Figure legends

**Figure 1.** Schematic representation of the FMDV genome and cDNA cassettes used in this study. All plasmids contain the T7 promotor. P1-2A: capsid precursor protein; 3C: $3C^{pro}$ wt or C142S mutant; IRES: internal ribosome entry site wild-type, GAGA or GTTA mutants; ATG: start codon; TGA: stop codon.

**Figure 2.** Expression and proteolytic processing of the FMDV capsid protein precursor P1-2A by $3C^{pro}$. BHK cells were infected with vaccinia virus vTF7-3 and transfected with plasmids containing the FMDV serotype O (a) or serotype A (b) cDNA cassettes. After 20 h, cell lysates were prepared and analysed by SDS-PAGE and immunoblotting using antisera specific for FMDV capsid proteins (top), FMDV $3C^{pro}$(middle, approx. 22 kDa) and β-actin (bottom, approx. 42 kDa). The presence of β-actin was used as a loading control. The results shown are representative of at least two independent experiments. Molecular mass markers (kDa) are indicated on the left.

**Figure 3.** Binding of expressed FMDV capsid proteins to serotype-specific anti-FMDV antibodies and to $\alpha_v\beta_6$ integrin. Samples were prepared using serotype O cDNA cassettes as described in Fig. 2 and equal amounts of cell lysates were analysed using a FMDV serotype O-specific antigen ELISA (a) and an ELISA for FMDV antigen bound to $\alpha_v\beta_6$ integrin (b). Samples were prepared using serotype A cDNA cassettes and analysed using a FMDV serotype A-specific antigen ELISA (c) and an ELISA for FMDV antigen bound to $\alpha_v\beta_6$ integrin (d). Results are presented as the mean from two independent experiments. Note: the samples were analysed in the same order as the samples in Fig. 2. AU, absorbance unit.

**Figure 4**. Characterization of FMDV protomers and assembled empty capsids. BHK cells were transfected as in Fig. 2 using the indicated FMDV cDNAs for serotype O (a, c) and serotype A (b, d). At 20 h post transfection, cell lysates were prepared and fractionated on a 10-30% sucrose gradient (a, b). The locations of protomers and empty capsids are indicated. FMDV proteins were detected using serotype-specific FMDV antigen ELISAs. AU, absorbance unit. (c, d) Aliquots of whole cell lysates and selected fractions containing protomers (fr. 3) and empty capsids (fr. 14) were analysed by SDS-PAGE and immunoblotting using antisera specific for all FMDV capsid proteins (top) or for VP2 alone (bottom). The results shown are representative of two independent experiments. Molecular mass markers (kDa) are indicated on the left.

**Figure 5**. Binding of FMDV protomers and assembled empty capsids to serotype-specific anti-FMDV antibodies and to $\alpha_v\beta_6$ integrin. (a, b) Fractions containing protomers and assembled empty capsids (serotype O and A, respectively) were assayed using FMDV antigen ELISAs for binding to $\alpha_v\beta_6$ integrin-coated plates in the absence (-EDTA) or presence (+EDTA) of the divalent cation chelator. Binding buffer was used as the control. Results are presented as mean ± SEM of triplicate samples. (c, d) Purified FMDV empty capsids (serotype O and A, respectively) were analysed using serotype-specific antigen ELISAs (c) and for their ability to bind to $\alpha_v\beta_6$ integrin (d). The results shown are representative of two independent experiments. AU, absorbance unit.

**Figure 6.** FMDV imaging and maps. (a) Electron micrograph of assembled FMDV serotype A empty capsids. BHK cells were infected with the vaccinia virus vTF7-3 and transfected with the serotype A FMDV P1-2A-IRESgtta3Cwt plasmid. At 20 h post transfection, cells were harvested and empty capsids were purified by sucrose gradient centrifugation and concentrated. The capsids

were stained with NanoVan and data collected by electron microscopy. Bar, 50 nm. (b) Surface-rendered three-dimensional reconstruction of FMDV serotype A empty capsids at a resolution of 36Å. The icosahedral asymmetric unit is indicated by the triangle. (c) For comparison, a low-resolution map was calculated from the X-ray crystal structure of FMDV serotype A1061 (Fry *et al.*, 2005) to a resolution of 8Å.

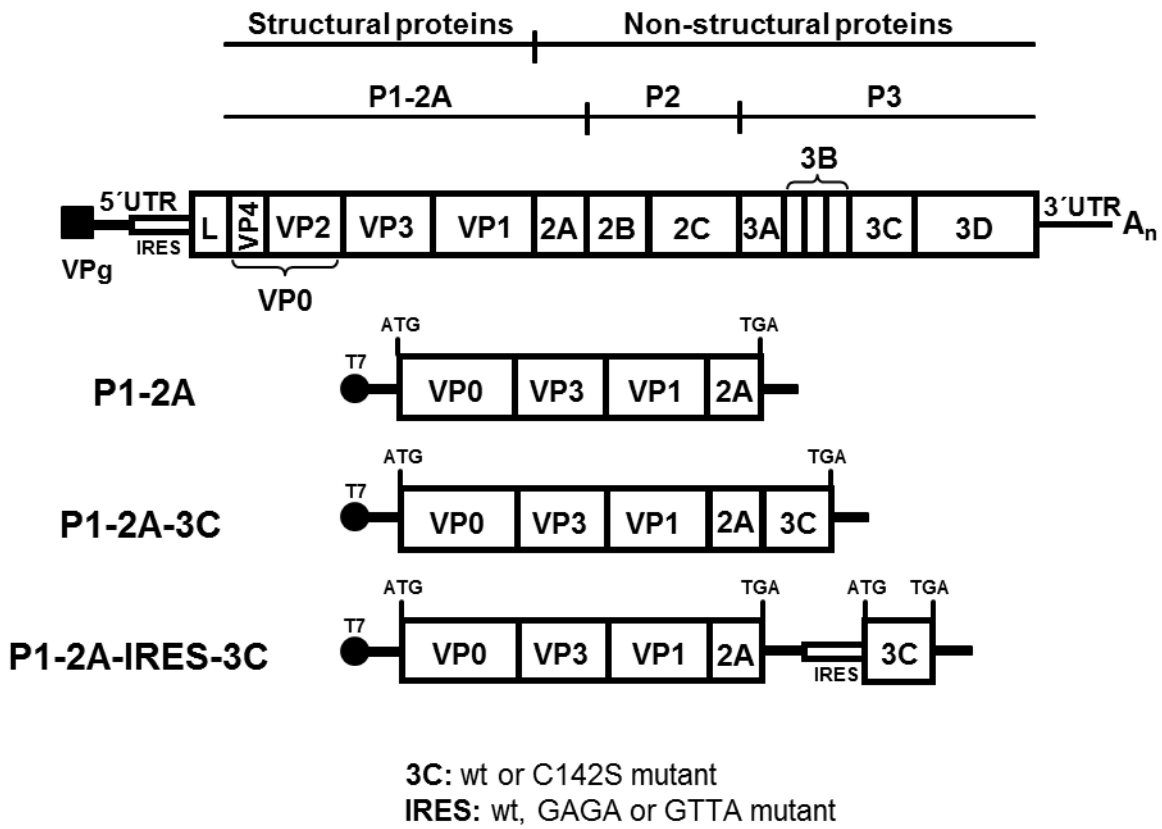


**3C:** wt or C142S mutant
**IRES:** wt, GAGA or GTTA mutant

Figure 1

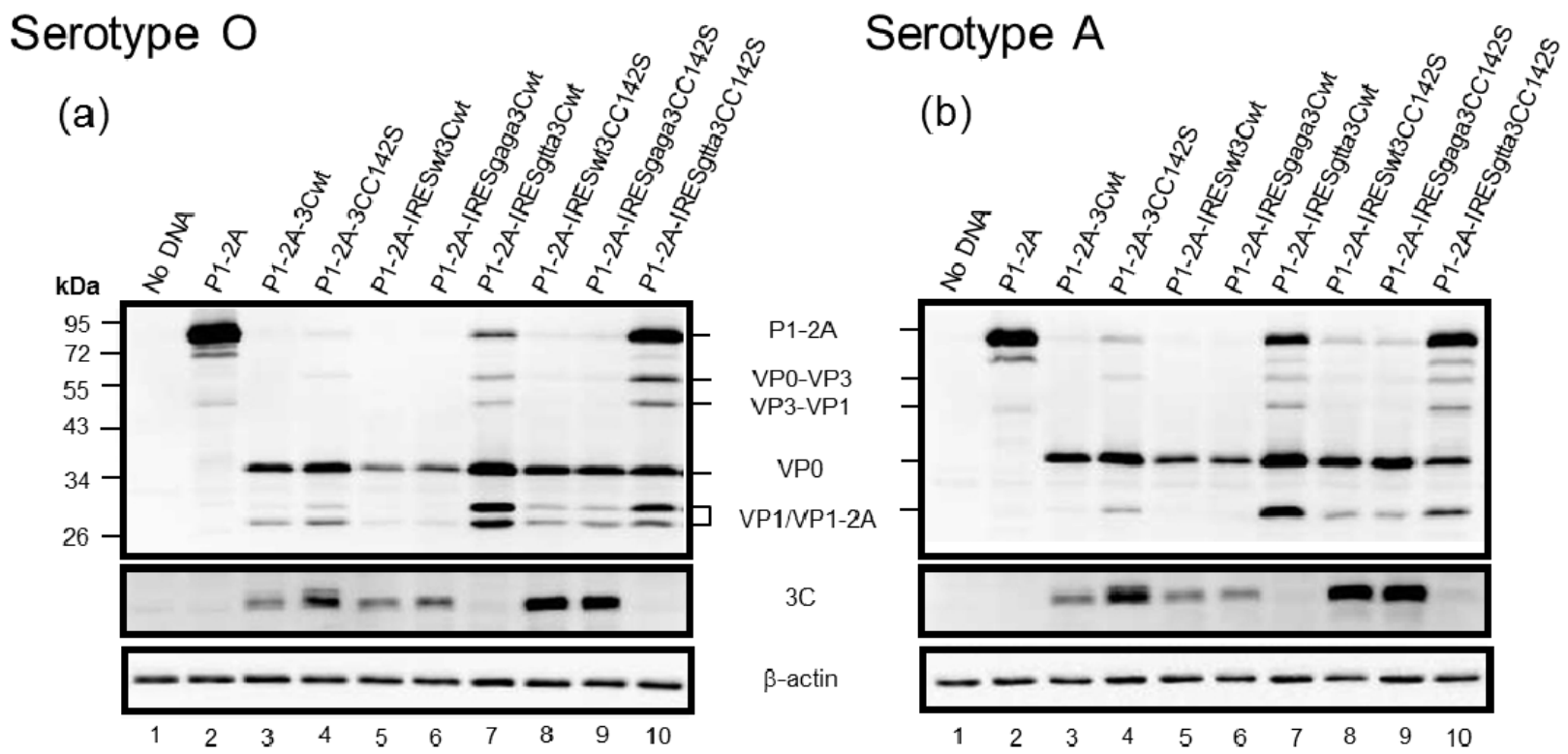
Serotype O
(a)
No DNA
P1-2A
P1-2A-3Cwt
P1-2A-3CC142S
P1-2A-IRESwt3Cwt
P1-2A-IRESgaga3Cwt
P1-2A-IRESgtta3Cwt
P1-2A-IRESwt3CC142S
P1-2A-IRESgaga3CC142S
P1-2A-IRESgtta3CC142S
kDa
95
72
55
43
34
26
P1-2A
VP0-VP3
VP3-VP1
VP0
VP1/VP1-2A
3C
β-actin
1 2 3 4 5 6 7 8 9 10
Serotype A
(b)
No DNA
P1-2A
P1-2A-3Cwt
P1-2A-3CC142S
P1-2A-IRESwt3Cwt
P1-2A-IRESgaga3Cwt
P1-2A-IRESgtta3Cwt
P1-2A-IRESwt3CC142S
P1-2A-IRESgaga3CC142S
P1-2A-IRESgtta3CC142S
1 2 3 4 5 6 7 8 9 10

Figure 2

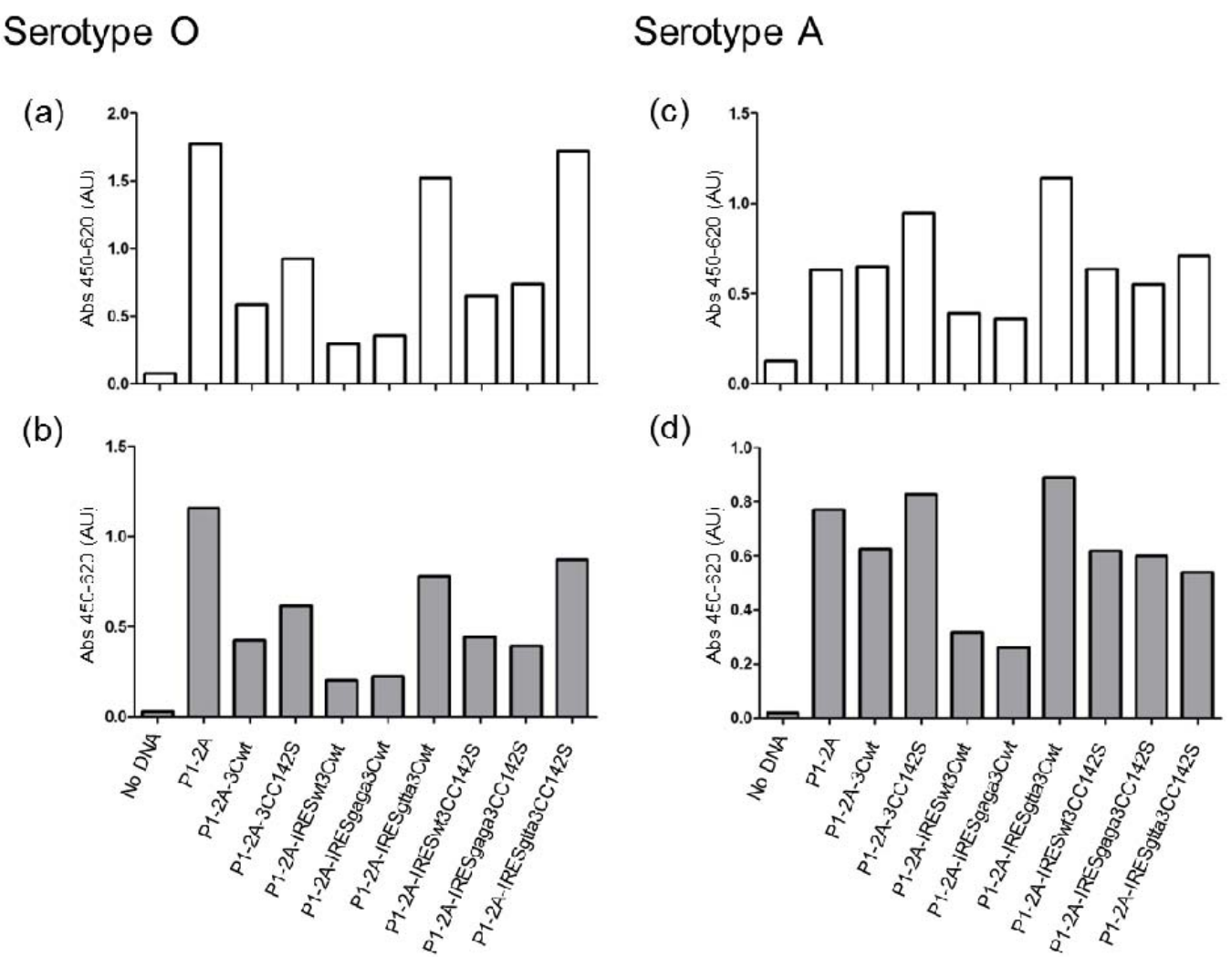
Serotype O
Serotype A
(a)
(b)
(c)
(d)
Abs 450-620 (AU)
No DNA
P1-2A
P1-2A-3Cwt
P1-2A-3CC142S
P1-2A-IRESwt3Cwt
P1-2A-IRESgaga3Cwt
P1-2A-IRESgtta3Cwt
P1-2A-IRESwt3CC142S
P1-2A-IRESgaga3CC142S
P1-2A-IRESgtta3CC142S

Figure 3

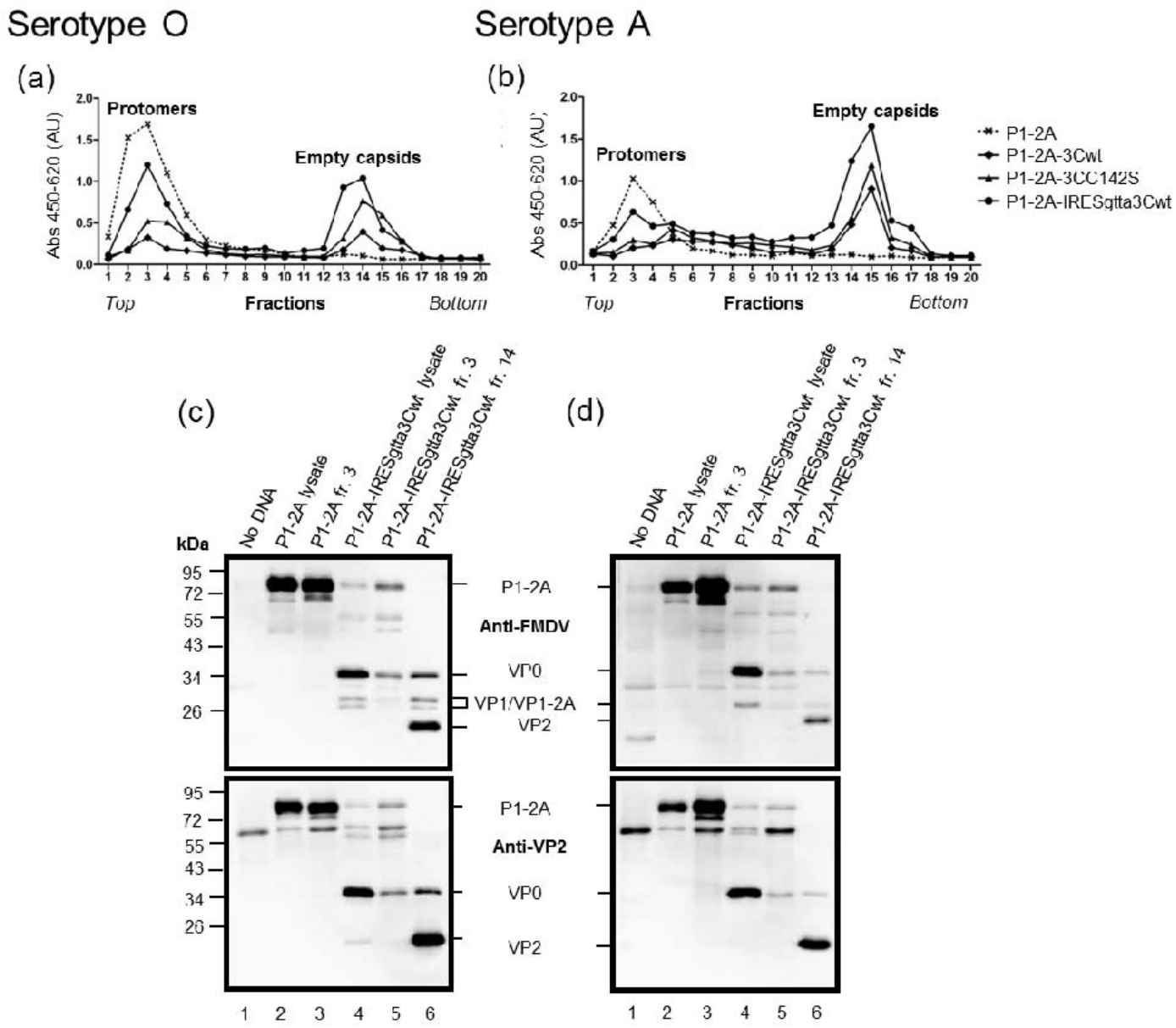
Serotype O
Serotype A
(a)
(b)
Protomers
Empty capsids
Abs 450-620 (AU)
Top
Fractions
Bottom
P1-2A
P1-2A-3Cwt
P1-2A-3CC142S
P1-2A-IRESgtta3Cwt
(c)
(d)
No DNA
P1-2A lysate
P1-2A fr. 3
P1-2A-IRESgtta3Cwt lysate
P1-2A-IRESgtta3Cwt fr. 3
P1-2A-IRESgtta3Cwt fr. 14
kDa
95
72
55
43
34
26
P1-2A
Anti-FMDV
VP0
VP1/VP1-2A
VP2
Anti-VP2
1 2 3 4 5 6

Figure 4

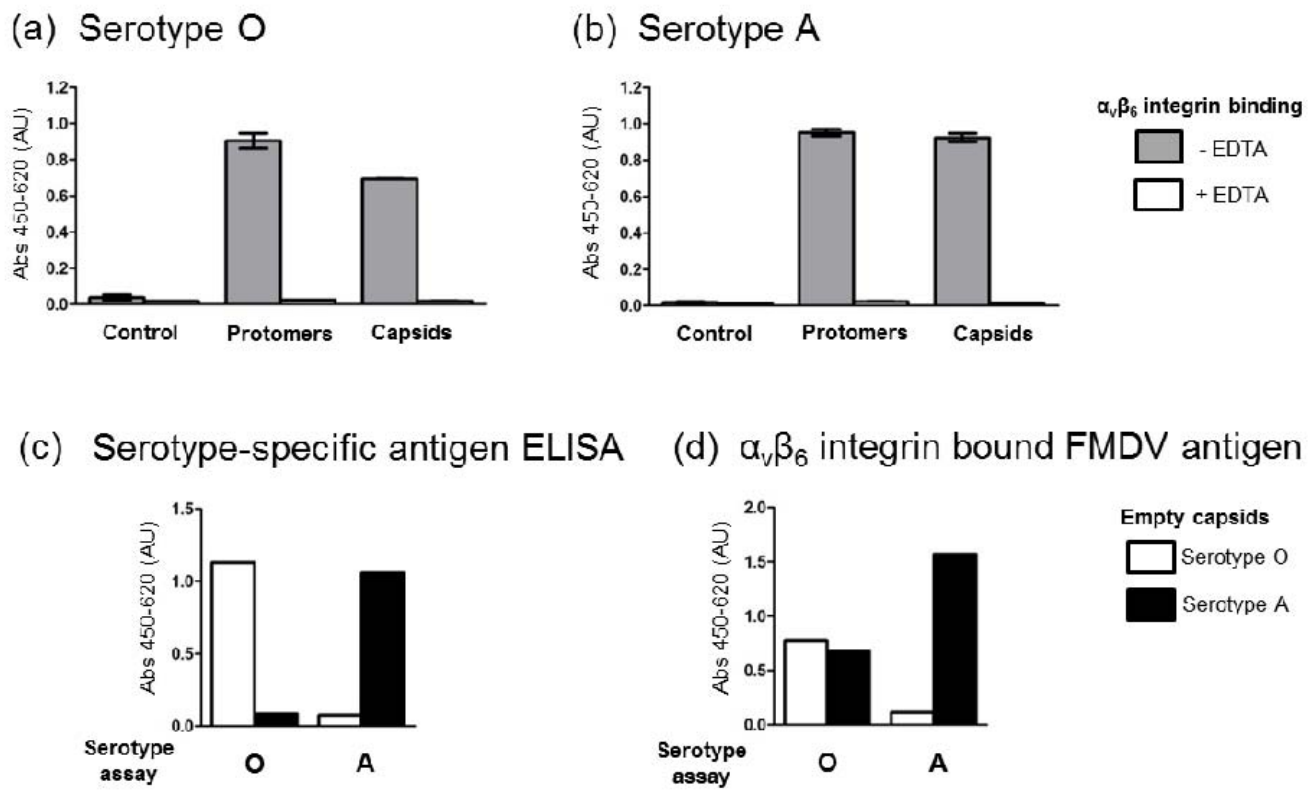
(a) Serotype O
(b) Serotype A
Abs 450-620 (AU)
1.2
1.0
0.8
0.6
0.4
0.2
0.0
Control
Protomers
Capsids
αvβ6 integrin binding
- EDTA
+ EDTA
(c) Serotype-specific antigen ELISA
(d) αvβ6 integrin bound FMDV antigen
1.5
0.5
2.0
1.5
Serotype assay
O
A
Empty capsids
Serotype O
Serotype A

Figure 5

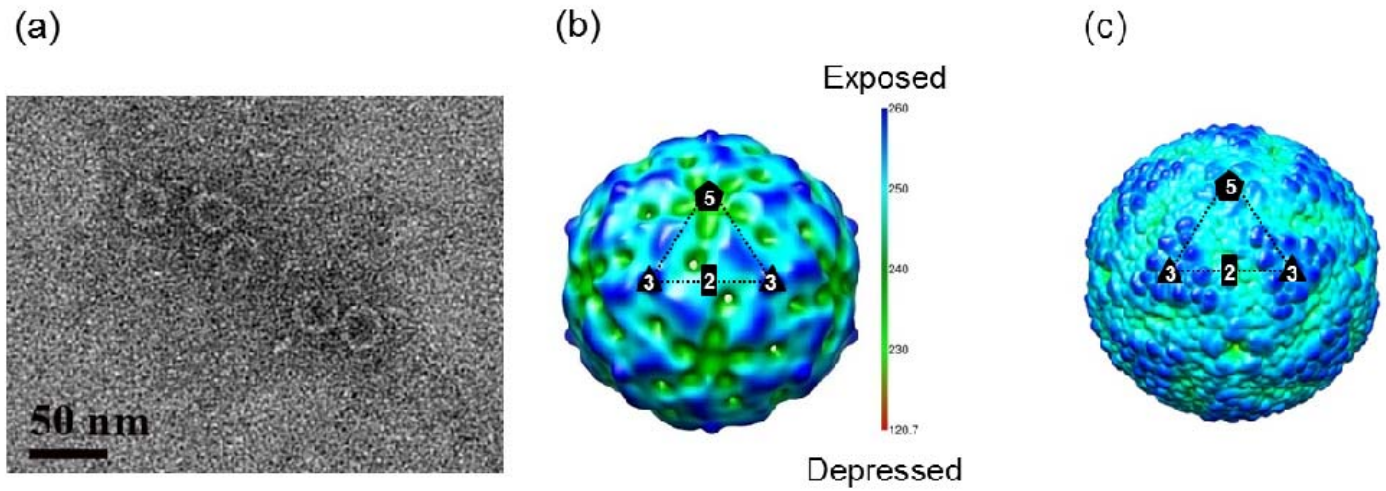


Figure 6